RSC Advances

Voltammetric studies on the inter-relationship of the redox chemistry of TTF, TTF•+, TTF2+ and HTTF+ in acidic media

Journal:	*RSC Advances*
Manuscript ID:	RA-ART-12-2014-016588.R1
Article Type:	Paper
Date Submitted by the Author:	27-Jan-2015
Complete List of Authors:	Adeel, Shaimaa; Monash University, Chemistry Abdelhamid, Muhammad; RMIT, Nafady, Ayman; Monash University, Chemistry Li, Qi; Monash University, Chemistry Martin, Lisandra; Monash University, Chemistry Bond, Alan; Monash University, Chemistry

Journal Name

RSCPublishing

ARTICLE

Voltammetric studies on the inter-relationship of the redox chemistry of TTF, $TTF^{\bullet+}$, TTF^{2+} and $HTTF^{+}$ in acidic media

Cite this: DOI: 10.1039/x0xx00000x

Received 00th January 2012,
Accepted 00th January 2012

DOI: 10.1039/x0xx00000x

www.rsc.org/

Shaimaa Adeel,[a] Muhammad E. Abdelhamid,[b] Ayman Nafady,[a,c] Qi Li,[a] Lisandra Martin,[a] and Alan Bond[a]

The electrochemistry of TTF, $TTF^{\bullet+}$, TTF^{2+} and $HTTF^{+}$ (TTF = tetrathiafulvalene) has been studied in acetonitrile (0.1 M Bu_4NPF_6) solutions containing ethereal HBF_4 or trifluoroacetic acid (TFA) using transient and steady-state voltammetric techniques. In the absence of acid, the oxidation of TTF occurs via two, diffusion controlled, chemically and electrochemically reversible, one-electron processes with reversible formal potentials of -74 and 311 mV vs $Fc^{0/+}$ (Fc = ferrocene). The voltammetry in the presence of acid is far more complex. Voltammetric and UV–vis data reveals that the parent TTF undergoes facile protonation to yield the structurally modified $HTTF^{+}$ cation in presence of acid. In contrast, detailed analysis of the data show that electrochemically generated $TTF^{\bullet+}$ and TTF^{2+} do not react with acid. The voltammetry in the presence of acid has been simulated to provide a thermodynamic and kinetic description of the acid–base chemistry coupled to electron transfer.

Introduction

Tetrathiafulvalene (TTF) chemistry has attracted significant interest since the discovery that the oxidized TTF^{+} form could be combined with suitable anions to give organic semi-conductors.[1] Since then, TTF and its derivatives have been used to develop sensors, superconductors, photovoltaic cells,[2-7] solar cells,[8-12] liquid crystals, gels[13-15] and recently used to facilitate the reduction of oxygen to water.[16] The electrochemical oxidation of TTF to $TTF^{+\bullet}$ and further to TTF^{2+} in aprotic media is now well established. However, the presence of acid should modify this redox chemistry since reaction of TTF with a Bronsted acid was shown to give $HTTF^{+}$ and the cation radical.[17] Protonation of the TTF molecule occurs at the central carbon-carbon double bond to give a substantial structural change as shown in equation 1. Giffard *et al.*[17-20] prepared the structurally characterised $(HTTF)BF_4$ by reaction of TTF with ethereal HBF_4 in $CHCl_3$.

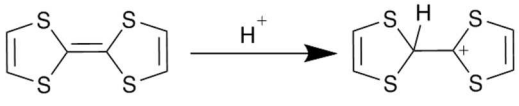

(1)

Despite substantial efforts to understand the oxidation of TTF, it is surprising that the effect of acid on the chemistry of TTF, and its oxidised $TTF^{+\bullet}$ and TTF^{2+} cations remains relatively neglected, particularly given the large number of applications proposed for technologies based on this redox active system. In this paper, a detailed investigation of the chemistries of TTF, $TTF^{+\bullet}$ and TTF^{2+} in the presence of acid is reported. Electrochemical techniques provide the primary source of information used to elucidate details of the $TTF^{0/+\bullet/2+}$ redox system and the interrelationships with $HTTF^{+}$. Non-aqueous acid (54% ethereal) HBF_4 and anhydrous trifluoroacetic acid (TFA) were chosen as the source of added proton in order to avoid the presence of water, which modifies the chemical and electrochemical behaviour of TTF.[21] Importantly, neither ethereal HBF_4 nor TFA are electroactive in the potential range where TTF redox chemistry occurs. A mechanism that accounts for the dependence of the voltammetry of TTF on the concentration of TFA and HBF_4 is proposed and supported by good agreement of simulated and experimental data.

Experimental Section

Materials

CH_3CN (HPLC grade, Merck) was distilled from calcium hydride and stored in a glove box. TTF (99%, Aldrich), 54% ethereal HBF4 (Aldrich), trifluoroacetic acid (TFA), 2-propanol (BDH), chloroform (MERCK) and acetone (MERCK) were

used as supplied by the manufacturer. The supporting electrolyte, tetrabutylammonium hexafluoro-phosphate (Bu_4NPF_6, 98%) was purchased from Wako Pure Chemical Industries, Japan and was recrystallized from ethanol, (95%) and vacuum dried before use.

Electrochemistry

Cyclic voltammetric measurements, under dry box conditions, were undertaken with a BAS100 electrochemical workstation interfaced to a standard three-electrode electrochemical cell configuration. Either a 3 mm diameter glassy carbon (GC), 1.6 mm diameter gold, 1.6 mm diameter platinum or a 12 μm diameter carbon fibre micro-disk were used as the working electrodes. These were polished with 0.3 μm aqueous alumina slurries, rinsed with distilled H_2O and acetone, and then dried with nitrogen gas prior to each measurement. Ag/Ag^+ (10 mM $AgNO_3$ in CH_3CN, 0.1 M Bu_4NPF_6) was used as the reference electrode and platinum wire as the counter electrode. Simulations of cyclic voltammograms were obtained using DigiSim 3.03 software.

Hydrodynamic voltammetric measurements with a 3mm GC diameter rotating disk electrode (RDE) were undertaken with the BAS100 electrochemical workstation combined with a BAS MF-2066 RDE electrode assembly and the same reference and auxiliary electrodes as used for cyclic voltammetry.

Bulk electrolysis experiments were used to generate the one- and two-electron oxidized species ($TTF^{+\bullet}$ and TTF^{2+}) in a three-compartment cell, with each compartment being separated by a fine glass frit to minimize solution mixing. A large-area carbon felt cloth (2×2 cm) (Tokai Carbon Japan) or a BAS GC basket net were used as working electrodes. Further details are available in our previous studies.[21]

All potentials are referred to the ferrocene ($Fc^{0/+}$) reference couple. Thus, the measured potential vs. Ag/Ag^+ was converted to the ferrocene scale via measurement of the reversible formal potential of the $Fc^{0/+}$ redox couple vs. Ag/Ag^+ under the relevant conditions. The potential of the Ag/Ag^+ reference electrode is - 85 mV vs. $Fc^{0/+}$.

UV-Vis Spectrophotometry

UV-Vis spectra were recorded on a Jasco Model V-670 spectrophotometer with a quartz cell having a 1 mm path length.

Results and Discussion

Voltammetry of TTF, $TTF^{\bullet+}$ and TTF^{2+} in acetonitrile

Cyclic voltammograms at a GC macrodisk electrode and near steady-state voltammograms obtained with a carbon fibre microelectrode or a GC rotating disc electrode for 1.0 mM TTF, 1.0 mM $TTF^{+\bullet}$ and 1.0 mM TTF^{2+} are shown in Figure 1. $TTF^{+\bullet}$ and TTF^{2+} solutions used in these experiments were quantitatively prepared by bulk oxidative electrolysis of TTF solutions in acetonitrile using an applied potential (E_{appl}) of 120 mV and 620 mV to generate TTF^{2+} (vs. $Fc^{0/+}$), respectively. This resulted in the persistent red coloured $TTF^{+\bullet}$, or yellow coloured TTF^{2+} solutions. TTF and its cations each give rise to the expected two, electrochemically reversible, one-electron processes. The half-wave potentials ($E_{1/2}$, where the current equals one-half of the limiting value in steady-state voltammetry), (Figure 1a,c) or the midpoint potentials (E_m) calculated from the average of the oxidation and reduction peak potentials recorded under transient conditions (Figure 1b) for the $TTF/TTF^{+\bullet}$ and $TTF^{+\bullet}/TTF^{2+}$ redox couples are essentially identical, irrespective of the initial redox level. $E_{1/2}$ and E_m values approximate to the reversible formal potential (E_f^0). Thus $E_m(1)$ = -74 mV and $E_m(2)$ = 311 mV vs $Fc^{0/+}$, respectively, so that these two processes are separated by $E_m(1) - E_m(2) = 385$ mV.[22-25]

From Figure 1, it is apparent on the basis of the magnitudes of the relevant limiting, or peak, current values that the diffusion coefficient (D) for TTF is larger than that of $TTF^{+\bullet}$ and TTF^{2+}. Diffusion coefficients D_{TTF}, $D_{TTF+\bullet}$ and D_{TTF2+} calculated from the near-steady-state voltammograms using the carbon fibre micro disc electrode and GC RDE electrode are summarized in Table S1. Diffusion coefficients were also calculated by analysis of the peak currents from voltammograms obtained at a GC macrodisk electrode over the scan rate range of 100 mV s^{-1} to 1000 mV s^{-1} and application of the Randles–Sevcik equation. These values agree well with those obtained from the steady state voltammetric experiments (Table S1) and data in our prior publication.[21]

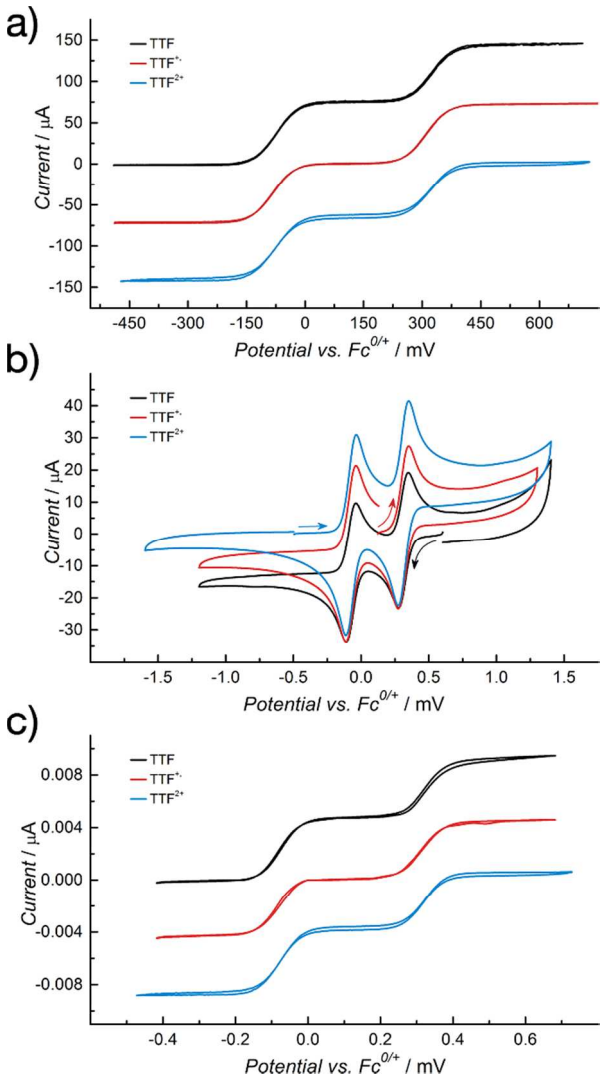

Figure 1. Voltammograms obtained from 1.0 mM TTF, $TTF^{+\bullet}$ and TTF^{2+} in acetonitrile (0.1 M Bu_4NPF_6) (a) near steady-state RDE voltammograms with a 3 mm diameter GC electrode (rotation rate = 2500 rpm, v = 20 mV s^{-1}, b) transient cyclic voltammograms with a 3.0 mm diameter GC macro-disc electrode (v = 100 mV s^{-1}) (c) near steady-state voltammograms with a 12.0 µm diameter carbon fibre micro-disc electrode (v = 20 mV s^{-1}).

Cyclic Voltammetry of TTF at a macrodisk electrode in acetonitrile in the presence of ethereal HBF_4

The cyclic voltammetry of 1 mM TTF in acetonitrile, changes dramatically upon the addition of 24.5 mM ethereal HBF_4. In particular, the $TTF^{0/+\bullet}$ and $TTF^{+\bullet/2+}$ oxidation processes almost completely vanish and are replaced by an irreversible oxidation process near 1000 mV (Figure 2). This new oxidation process has similar characteristics to that found in the voltammetry of TTF after addition of 10 % water to an acetonitrile (0.1 M Bu_4NPF_6) solution[21] and is assigned to the oxidation of $HTTF^+$. As expected, the same process is present in voltammograms of $(HTTF)BF_4$.[21] When diethyl ether was added to a 1.0 mM TTF solution, the voltammograms remained unaltered, implying that diethyl ether is not electroactive in the potential region of interest.

The conclusion that very little neutral TTF or its oxidised form remains present in bulk solution after addition of 24.5 mM HBF_4 is reached on the basis that the peak current magnitudes for the $TTF^{0/+\bullet/2+}$ processes are small when the potential is switched prior to oxidation of $HTTF^+$ at 620 mV (Figure 2). In contrast, when the potential is switched at 1320 mV after oxidation of HTTF, the $TTF^{2+/+\bullet}$ and $TTF^{+\bullet/0}$ processes are substantially recovered on reversing the potential scan direction. This implies that oxidation of $HTTF^+$ results in the formation of $TTF^{+\bullet}$ and H^+ and occurs in accordance with equations 2 and 3. However at this very positive switching potential of 1320 mV, $TTF^{+\bullet}$ will be immediately oxidized to TTF^{2+}, which is then reduced back to the neutral form via two, one-electron reduction processes on reversing the scan direction in cyclic voltammograms (Figure 2). Cyclic voltammograms at Au and Pt electrodes, in the presence of 24.5 mM ethereal HBF_4, are similar to those at a GC electrode (Figure S1) implying that the surface is not significant. Peak current magnitude differences in Figure S1 are associated with electrode area variation. Moreover, cyclic voltammograms for TTF in acetonitrile containing 24.5 mM ethereal HBF_4 are fully reproducible for at least one hour (Figure S2), suggesting that $HTTF^+$ is very stable under these conditions.

$$HTTF^+ \rightleftharpoons HTTF^{2+\bullet} + e^- \quad (2)$$

$$HTTF^{2+} \rightleftharpoons TTF^{+\bullet} + H^+ \quad (3)$$

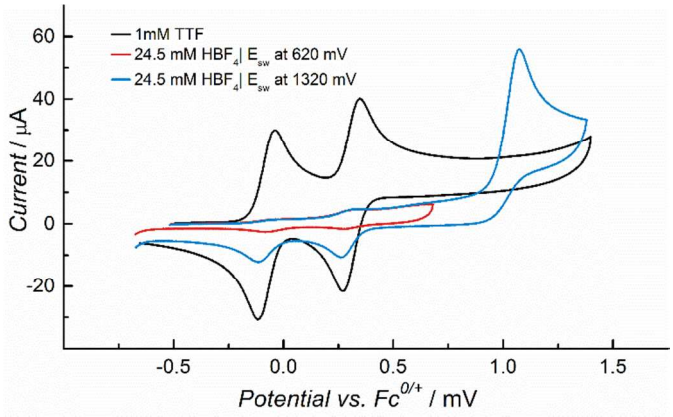

Figure 2. Cyclic voltammograms for 1.0 mM TTF in acetonitrile (0.1 M Bu_4NPF_6) before and after the addition of 24.5 mM ethereal HBF_4 at a GC electrode. Switching potentials (E_{sw}) are 620 mV and 1320 mV and scan rate is 100 mV s^{-1}.

Steady State Voltammetry of TTF in acetonitrile in the presence of ethereal HBF_4

Figure 3 illustrates the changes that take place in the steady state voltammetry at a 12 µm diameter carbon fibre electrode for the oxidation of 5.0 mM TTF in acetonitrile (0.1 mM Bu_4NPF_6) upon addition of acid. The limiting currents for both

the $TTF^{0/+\bullet}$ and $TTF^{+\bullet/2+}$ oxidation processes progressively decrease as the acid concentration is increased and are replaced by an irreversible oxidation process. Moreover, since the initial current becomes negative, rather than zero, in the presence of acid, it can be deduced that a small concentration of $TTF^{+\bullet}$ is now present, rather than exclusively the non-protonated TTF, which is in agreement with the conclusion reported by Giffard.[17] Cyclic voltammetry (see above) does not readily allow a decision to be made as to whether TTF, $TTF^{+\bullet}$ or TTF^{2+} are present after addition of acid.

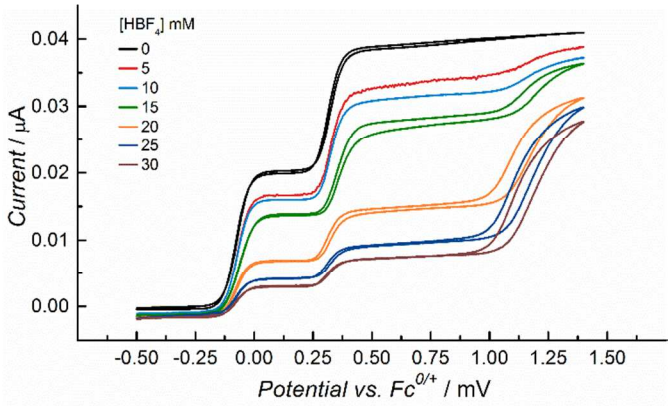

Figure 3. Steady-state voltammograms at a 12.0 µm diameter carbon fibre microelectrode (scan rate of 20 mV s^{-1}) obtained for 5.0 mM TTF on addition of designated ethereal HBF_4 concentrations.

The influence of HBF_4 on the voltammetry of $TTF^{+\bullet}$

The cyclic voltammetry of $TTF^{+\bullet}$ in the presence of ethereal HBF_4 also was explored. Figure 4 reveals that the addition of ethereal HBF_4 does not significantly alter the $TTF^{+\bullet/2+}$ oxidation process; i.e. E_m is independent of the acid concentration and full chemical reversibility of this process is retained. In contrast, the reversibility of the $TTF^{+\bullet/0}$ process is dramatically decreased. Significantly, the reduction peak current (i_p^{red1}) for this process does not markedly change with increasing concentration of ethereal HBF_4, whereas its oxidation counterpart, i_p^{ox1} decreases markedly. These cyclic voltammetric results imply that unlike neutral TTF, the radical cation $TTF^{+\bullet}$ does not react with acid.

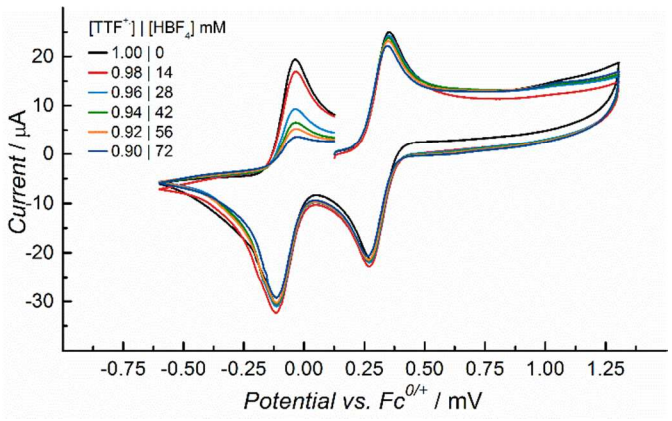

Figure 4. Cyclic voltammograms obtained at scan rate of 100 mV s^{-1} in acetonitrile (0.1 M Bu_4NPF_6) for $TTF^{+\bullet}$ with a 3 mm diameter GC electrode at designated TTF and ethereal HBF_4 concentrations.

The influence of HBF_4 on the voltammetry of TTF^{2+}

The cyclic voltammetry of TTF^{2+} in the absence and the presence of ethereal HBF_4 is shown in Figure 5 and reveals that the addition of acid does not significantly alter the E_m value or chemical reversibility of the $TTF^{2+/+\bullet}$ process. In contrast, the chemical reversibility of the $TTF^{+\bullet/0}$ process is again affected by reaction of TTF with H^+. Thus, i_p^{ox1} decreases while i_p^{red1} remains essentially unchanged and a new irreversible oxidation process associated with generation of $HTTF^+$ appears at 1000 mV.

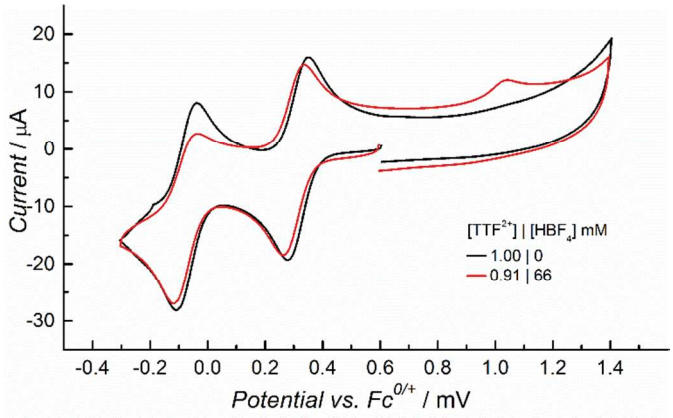

Figure 5. Cyclic voltammograms obtained at scan rate of 100 mV s^{-1} in acetonitrile (0.1 M Bu_4NPF_6) for TTF^{2+} in the absence and presence of ethereal HBF_4 at a GC electrode.

The above results lead to the conclusion that TTF^{2+}, like $TTF^{+\bullet}$ does not react with acid. In accordance with this hypothesis, cyclic voltammograms of TTF^{2+} are highly dependent on the switching potential in the presence of acid (Figure S3). Thus, when the potential is switched at 140 mV, the $TTF^{2+/+\bullet}$ process is unaffected and no irreversible oxidation peak is detected at 1000 mV. In contrast, when the switching potential is at -300 mV (i.e. more negative than for the $TTF^{+\bullet/0}$ process), the chemical reversibility of the $TTF^{0/+\bullet}$ process diminishes and the irreversible $HTTF^{2+}$ oxidation process appears, consistent with the conclusion that the irreversible oxidation process arises from protonation of TTF rather than TTF^{2+}.

In order to further confirm that the species responsible for the irreversible process at positive potentials is due to oxidation of $HTTF^+$ formed by protonation of TTF, an acidic solution of TTF^{2+} was reduced by exhaustive bulk electrolysis conditions, back to neutral TTF by applying a controlled potential of -300 mV, i.e. sufficiently negative to convert all of the TTF^{2+} to neutral TTF. The cyclic voltammogram obtained after this exhaustive reductive electrolysis experiment (Figure 6) shows that all regenerated TTF has reacted with acid to form $HTTF^+$. Furthermore, the reduction components of the $TTF^{2+/+\bullet}$ and $TTF^{+\bullet/0}$ processes are regenerated when $HTTF^+$ is oxidized to $HTTF^{2+}$ which loses the proton to form $TTF^{\bullet+}$, which in turn is

oxidized to TTF^{2+} at this very positive potential. This is followed by reduction back to TTF via $TTF^{+\bullet}$ in the negative potential scan direction of cyclic voltammograms. Once again these data imply that only neutral TTF reacts with acid and that oxidation of $HTTF^{+\bullet}$ leads to $TTF^{+\bullet}$ and H^+.

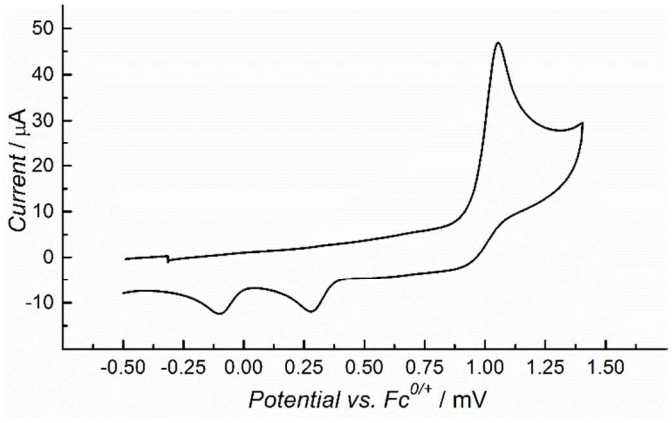

Figure 6. Cyclic voltammogram obtained for the oxidation of $HTTF^+$ generated by reductive electrolysis of 0.91 mM TTF^{2+} in acetonitrile (0.1 M Bu_4NPF_6) solution containing of 66 mM HBF_4. A 3 mm GC electrode and a scan rate of 100 mV s^{-1} was used.

After exhaustive reductive electrolysis of TTF^{2+} in the presence of 66 mM HBF_4, the second cycle of potential (Figure S4) gives rise to $TTF^{0/+\bullet}$ and $TTF^{+\bullet/2+}$ oxidation components. These results imply that protonation of TTF by H^+ (equation 1) is a moderately slow process on the cyclic voltammetric time scale; 100 mV s^{-1} in the case of Figure 4.

The Voltammetry of TTF in acetonitrile in the presence of TFA

In order to gain additional insights into the mechanism associated with the acidification reaction, the weak acid TFA, rather than strong acid, HBF_4, was added to an acetonitrile solution containing TTF and the reaction was monitored using voltammetry and UV-visible spectrometry. Under dry box conditions, both the $TTF^{0/+\bullet}$ and $TTF^{+\bullet/2+}$ oxidation processes again are replaced by an irreversible $HTTF^+$ oxidation process at more positive potential upon addition of TFA, as shown in Figure S5. However, higher concentrations of TFA are required to achieve the same impact as observed with the stronger, HBF_4 acid. The peak potentials obtained from the positive potential scan direction in cyclic voltammograms for 4.3 mM TTF in the presence of 1.5 M TFA (Figure S6) are almost independent of the scan rate after allowance is made for the Ohmic, iR_u (where i = current, R_u = uncorrected resistance) drop. Moreover, the oxidation peak currents for the $TTF^{0/+\bullet}$, $TTF^{+\bullet/2+}$ and $HTTF^+$ processes are all proportional to the square root of the scan rate, $v^{1/2}$ and pass through the origin implying that all are diffusion controlled processes (Figure S7).

UV-visible spectra of TTF, $TTF^{+\bullet}$ and TTF^{2+} in the presence of TFA

The UV-visible spectra of 0.17 mM TTF, $TTF^{+\bullet}$ and TTF^{2+} were monitored in acetonitrile (0.1 M Bu_4NPF_6) by the UV-vis spectrophotometry under similar conditions used for the voltammetric studies. Results are displayed in Figure 7. No change in the UV-visible spectra for the $TTF^{+\bullet}$ and TTF^{2+} cases were evident following addition of TFA. In contrast, the UV-vis spectra for TTF charged markedly as $HTTF^+$ was formed. Thus, the TTF absorption bands with λ_{max} at 303 and 317 nm decreased.[21] The new band that appears at 233 nm corresponds to the formation of $HTTF^+$. Two additional new absorption bands with λ max at 435 nm and 580 nm correspond to formation of a small amount of $TTF^{\bullet+}$. These results are fully consistent with voltammetric data. The origin of the small side reaction to produce $TTF^{+\bullet}$ has been attributed to the reaction of $HTTF^+$ with TTF to give $HTTF^\bullet$ and $TTF^{+\bullet}$.[17] Under dry box conditions used in this study, the amount of $TTF^{+\bullet}$ found is very small and reaction with adventitious water also may be involved in generation of $TTF^{+\bullet}$.

The time dependence of the evolution of $HTTF^+$ and $TTF^{+\bullet}$ on addition of acid was monitored by UV-vis spectrophotometry. Results in Figure S8 for 0.25 mM TTF in acetonitrile (0.1 M Bu_4NPF_6) upon addition of 500 mM TFA show that the absorption bands for neutral TTF, at 303 and 307 nm, rapidly decrease to 62% of the initial value, in the first 5 minutes of the reaction time. These absorption bands are replaced by those characteristic of $HTTF^+$ (233 nm) and $TTF^{+\bullet}$ (435 and 580 nm). However, from 20 min to 75 hrs, the absorbance remains almost constant, indicating the completion of the reaction occurs fairly rapidly. Clearly, the final product on this long timescale is still predominantly $HTTF^+$ rather than $TTF^{+\bullet}$.

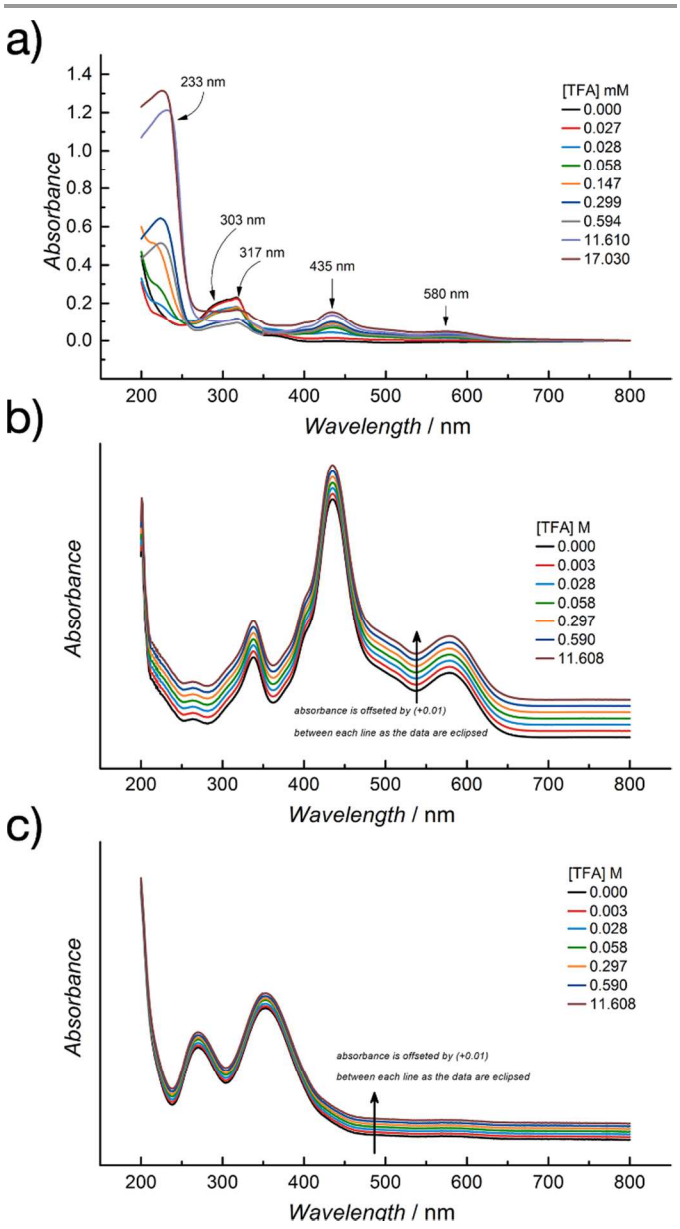

Figure 7. UV-vis spectra, obtained upon addition of designated TFA concentration to 0.17 mM (a) TTF, (b) $TTF^{+\bullet}$ and (c) TTF^{2+} in acetonitrile (0.1 M Bu_4NPF_6).

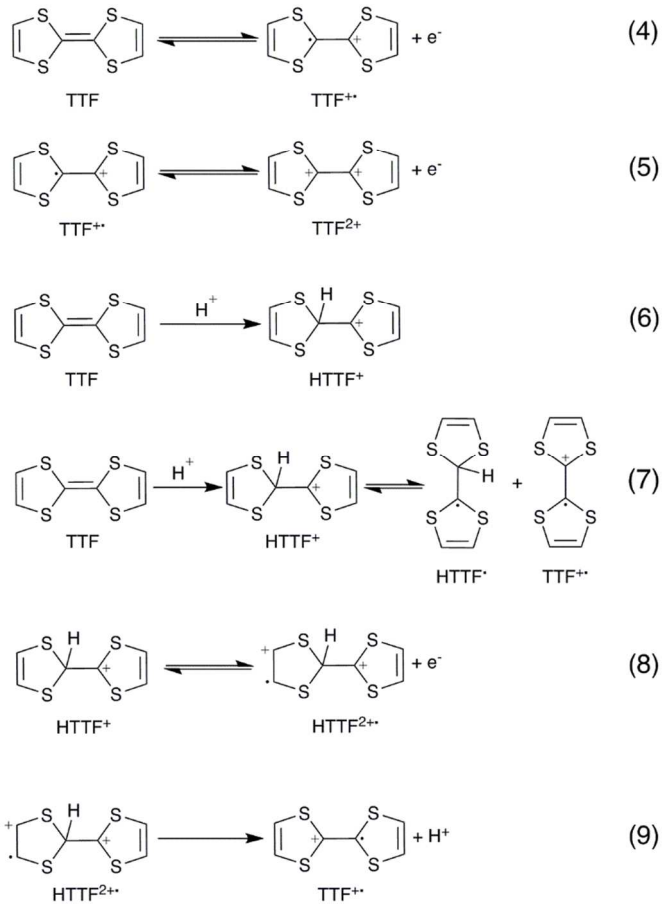

Simulations of the voltammetry of TTF in the presence of acid

All voltammetric data obtained upon addition of acid to a TTF solution in acetonitrile lead to the following conclusions: (i) neutral TTF reacts rapidly with ethereal HBF_4 or TFA acid to form $HTTF^+$ (ii) neither the $TTF^{+\bullet}$ cation radical nor the TTF^{2+} dication reacts with acid, although $HTTF^+$ may react with neutral TTF to form $TTF^{+\bullet}$ and $HTTF^{\bullet}$, as reported by Giffard *et al.*,[17] and (iii) under voltammetric conditions $HTTF^+$ is oxidized to $HTTF^{2+\bullet}$, which subsequently loses a proton to generate $TTF^{+\bullet}$ that can be oxidised to TTF^{2+}. On the basis of these findings, a mechanism that describes the voltammetry of TTF in acid is summarised by equations 4 to 9.

Simulations in the presence of HBF_4 based on this mechanism, using parameters; T = 293 K, D_{TTF} = 2.2 x 10^{-5} cm^2 s^{-1}, $D_{TTF\bullet+}$ = 1.9 x 10^{-5} cm^2 s^{-1}, D_{TTF2+} = 1.6 x 10^{-5} cm^2 s^{-1}, D_{H+} = 3.0 x 10^{-3} cm^2 s^{-1}; area of electrode = 0.0715 cm^2; R_u = 300 Ω, C_{dl} = 9 x 10^{-6} F (Table 1) are consistent with experimental cyclic voltammetric data, as shown in Figure 8. HBF_4 is assumed to be a strong acid and fully dissociated in CH_3CN. k_s values of 0.7, 0.5 and 0.3 cm s^{-1} with α = 0.5 were used for the heterogeneous electron transfer rates.[26] However, simulations were insensitive to variation of these electrode kinetic parameters as all electron transfer processes are essentially reversible on the time scale used. Futhermore, the double layer capacitance, C_{dl} = 9.0 x 10^{-6} F was assumed to be independent of potential, which clearly is not correct and is the origin of discrepancies between simulated and experimental current magnitude data, particularly at positive potentials. Other issues of sensitivity also arise. Additionally, equation 7 makes little contribution to the simulation and could be neglected, so values of parameters related to this are not significant. Similar considerations apply to equation 9, where the key consideration is that the equilibrium position lies far to the right and the rate of proton loss has to be very fast. In summary, the simulations support the mechanism proposed but no unique combination of all the parameters has been achieved.

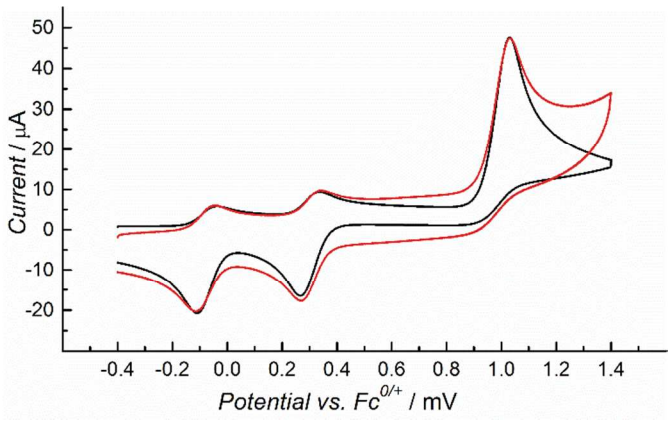

Figure 8. Comparison of simulated (black) and experimental (red) cyclic voltammograms obtained for 1.0 mM TTF in acetonitrile (0.1 M Bu_4NPF_6) in the presence of 10 mM ethereal HBF_4. A scan rate of 100 mV s^{-1} with a 3 mm diameter GC electrode was used.

Table 1. Parameters that simulate the mechanism proposed in equations 4 to 9, to describe the voltammetry of TTF in acetonitrile (0.1 M Bu_4NPF_6) solutions containing ethereal HBF_4.[a,b,c]

Reaction	E° / V	k_s / cm s^{-1}	K_{eq}	k_f
$T = T^{+\bullet} + e$	-0.071	0.7		
$T^{+\bullet} = T^{2+} + e$	0.317	0.3		
$HB = H^+ + B^-$			0.01	100
$T + H^+ = HT^+$			1000	40
$HT^+ + T = T^{+\bullet} + HT^\bullet$			1×10^{-7}	0.02
$HT^+ = HT^{2+\bullet} + e$	1.034	0.5		
$TH^{2+\bullet} = T^{+\bullet} + H^+$			5.4×10^{14}	4×10^6

a) T = TTF, $T^{+\bullet}$ = $TTF^{+\bullet}$, T^{2+} = TTF^{2+}, HB = HBF_4, TH^+ = $HTTF^+$, $HT^\bullet$ = $HTTF^\bullet$ and $HT^{2+\bullet}$ = $HTTF^{2+}$, K_{eq} = equilibrium constant and k_f = forward rate constant for the designated reaction

b) Other parameters used in simulation are given in the text

c) Units of K_{eq} and k_f depend on the reaction

Conclusion

The interrelationships of the redox chemistry of TTF, $TTF^{+\bullet}$, TTF^{2+} and $HTTF^+$ have been studied in the presence and the absence of a strong acid, HBF_4 and a weak acid, TFA in acetonitrile (0.1 M Bu_4NPF_6) using voltammetric and UV-vis spectrophotometry. In the absence of acid, the voltammetry of TTF is simple and gives rise to, two well-resolved diffusion controlled, chemically and electrochemically reversible one-electron processes. The E^o values for the $TTF^{0/+\bullet}$ and $TTF^{+\bullet/2+}$ couples are -0.74 and 0.31 V vs Fc/Fc^+, respectively. On addition of acid, TTF reacts with H^+ to form $HTTF^+$. In contrast, $TTF^{+\bullet}$ and TTF^{2+} do not react with acid. Oxidation of $HTTF^+$ is assumed to generate $HTTF^{2+\bullet}$ which then rapidly deprotonates to give $TTF^{+\bullet}$. Addition of acid to TTF also gives a small quantity of $TTF^{+\bullet}$ in a side reaction. Simulations based on the postulated mechanism are in good agreement with experimental voltammetric behaviour of TTF in the presence of acid.

Acknowledgements

AMB and LLM gratefully acknowledge financial support from the Australian Research Council. SA gratefully acknowledges funding from a Monash Graduate Scholarship.

Notes

[a] School of Chemistry, Monash University, Clayton, Victoria 3800, Australia. *E-mails: Lisa.Martin@monash.edu, Alan.Bond@monash.edu*

[b] School of Applied Sciences, RMIT University, GPO Box 2476V, Melbourne, 3001, Australia.

[c] Current address: King Saud University, College of Science, Department of Chemistry, PO Box 2455, Riyadh 11451, Saudi Arabia.

† Electronic Supplementary Information (ESI) available. See DOI: 10.1039/b000000x/

References

1. J. L. Segura and N. Martín, *Angewandte Chemie International Edition*, 2001, **40**, 1372-1409.
2. K. Iliopoulos, R. Czaplicki, H. El Ouazzani, J. Y. Balandier, M. Chas, S. Goeb, M. Salle, D. Gindre and B. Sahraoui, *Applied Physics Letters*, 2010, **97**, 101104-101103.
3. I. Fuks-Janczarek, J. Luc, B. Sahraoui, F. Dumur, P. Hudhomme, J. Berdowski and I. V. Kityk, *Journal of Physical Chemistry B*, 2005, **109**, 10179-10183.
4. B. Sahraoui, X. Nguyen Phu, T. Nozdryn and J. Cousseau, *Synthetic Metals*, 2000, **115**, 261-264.
5. K. Sako, M. Kusakabe, H. Fujino, S. X. Feng, H. Takemura, T. Shinmyozu and H. Tatemitsu, *Synthetic Metals*, 2003, **137**, 899-900.
6. K. Uchida, G. Masuda, Y. Aoi, K. Nakayama and M. Irie, *Chemistry Letters*, 1999, 1071-1072.
7. T. Ishiguro, K. Yamaji and G. Saito, *Organic Superconductors, Second Edition*, Springer, 1998.
8. Y. Hou, Y. Chen, Q. Liu, M. Yang, X. Wan, S. Yin and A. Yu, *Macromolecules*, 2008, **41**, 3114-3119.
9. K. B. Simonsen, V. V. Konovalov, T. A. Konovalova, T. Kawai, M. P. Cava, L. D. Kispert, R. M. Metzger and J. Becher, *Journal of the Chemical Society, Perkin Transactions 2: Physical Organic Chemistry*, 1999, 657-666.
10. R. Berridge, P. J. Skabara, C. Pozo-Gonzalo, A. Kanibolotsky, J. Lohr, J. J. W. McDouall, E. J. L. McInnes, J. Wolowska, C. Winder, N. S. Sariciftci, R. W. Harrington and W. Clegg, *J. Phys. Chem. B*, 2006, **110**, 3140-3152.
11. M. A. Herranz and N. Martín, *Organic Letters*, 1999, **1**, 2005-2007.
12. Y. Geng, F. Pop, C. Yi, N. Avarvari, M. Gratzel, S. Decurtins and S.-X. Liu, *New J. Chem.*, 2014, **38**, 3269-3274.
13. J. Bigot, B. Charleux, G. Cooke, F. o. Delattre, D. Fournier, J. l. Lyskawa, L. n. Sambe, F. o. Stoffelbach and P. Woisel, *Journal of the American Chemical Society*, 2010, **132**, 10796-10801.
14. T. Akutagawa, K. Kakiuchi, T. Hasegawa, S.-i. Noro, T. Nakamura, H. Hasegawa, S. Mashiko and J. Becher, *Angewandte Chemie International Edition*, 2005, **44**, 7283-7287.
15. I. Danila, F. Riobe, J. Puigmarti-Luis, A. Perez del Pino, J. D. Wallis, D. B. Amabilino and N. Avarvari, *J. Mater. Chem.*, 2009, **19**, 4495-4504.

16. A. J. Olaya, P. Ge, J. r. m. F. Gonthier, P. Pechy, C. m. Corminboeuf and H. H. Girault, *Journal of the American Chemical Society*, 2011, **133**, 12115-12123.
17. M. Giffard, P. Frere, A. Gorgues, A. Riou, J. Roncali and L. Toupet, *J. Chem. Soc., Chem. Commun.*, 1993, 944-945.
18. M. Giffard, P. Alonso, J. Garin, A. Gorgues, T. P. Nguyen, P. Richomme, A. Robert, J. Roncali and S. Uriel, *Adv. Mater.* , 1994, **6**, 298-300.
19. M. Giffard, A. Gorgues, A. Riou, J. Roncali, T. P. Nguyen, J. Garín, S. Uriel and P. Alonso, *Synthetic Metals*, 1995, **70**, 1133-1134.
20. M. Giffard, M. Sigalov, V. Khodorkovsky, A. Gorgues and G. Mabon, *Synthetic Metals*, 1999, **102**, 1713-1713.
21. S. M. Adeel, Q. Li, A. Nafady, C. Zhao, A. I. Siriwardana, A. M. Bond and L. L. Martin, *RSC Advances*, 2014, **4**, 49789-49795.
22. Q. Li, C. Zhao, A. M. Bond, J. F. Boas, A. G. Wedd, B. Moubaraki and K. S. Murray, *Journal of Materials Chemistry*, 2011, **21**, 5398-5407.
23. D. L. Coffen, J. Q. Chambers, D. R. Williams, P. E. Garrett and N. D. Canfield, *Journal of the American Chemical Society*, 1971, **93**, 2258-2268.
24. Q. Li, J. Lu, J. F. Boas, D. A. K. Traore, M. C. J. Wilce, F. Huang, L. L. Martin, T. Ueda and A. M. Bond, *Inorganic Chemistry*, 2012, **51**, 12929-12937.
25. S. J. Shaw, F. Marken and A. M. Bond, *Electroanalysis*, 1996, **8**, 732-741.
26. A. M. Bond, K. Bano, S. Adeel, L. L. Martin and J. Zhang, *ChemElectroChem*, 2013, **1**, 99-107.

